



OPEN

Polluted dust promotes new particle formation and growth

SUBJECT AREAS:

ATMOSPHERIC SCIENCE
ATMOSPHERIC CHEMISTRYWei Nie^{1,2,6}, Aijun Ding^{1,6}, Tao Wang^{2,3}, Veli-Matti Kerminen⁴, Christian George⁵, Likun Xue³, Wenxing Wang², Qingzhu Zhang², Tuukka Petäjä⁴, Ximeng Qi^{1,6}, Xiaomei Gao², Xinfeng Wang², Xiuqun Yang^{1,6}, Congbin Fu^{1,6} & Markku Kulmala⁴

Received

22 April 2014

Accepted

22 August 2014

Published

16 October 2014

Correspondence and requests for materials should be addressed to A.D. (dingaj@nju.edu.cn) or T.W. (tao.wang@polyu.edu.hk)

¹Institute for Climate and Global Change Research & School of Atmospheric Sciences, Nanjing University, Nanjing, 210093, China, ²Environment Research Institute, Shandong University, Jinan, China, ³Department of Civil and Environmental Engineering, The Hong Kong Polytechnic University, Hong Kong, China, ⁴Division of Atmospheric Sciences, Department of Physics, University of Helsinki, Helsinki, Finland, ⁵Université de Lyon, Lyon, F-69626, France; Université Lyon 1, Lyon, F-69626, France; CNRS, UMR5256, IRCELYON, Institut de Recherches sur la Catalyse et l'Environnement de Lyon, Villeurbanne, F-69626, France, ⁶Collaborative Innovation Center of Climate Change, Jiangsu Province, China.

Understanding new particle formation and their subsequent growth in the troposphere has a critical impact on our ability to predict atmospheric composition and global climate change. High pre-existing particle loadings have been thought to suppress the formation of new atmospheric aerosol particles due to high condensation and coagulation sinks. Here, based on field measurements at a mountain site in South China, we report, for the first time, in situ observational evidence on new particle formation and growth in remote ambient atmosphere during heavy dust episodes mixed with anthropogenic pollution. Both the formation and growth rates of particles in the diameter range 15–50 nm were enhanced during the dust episodes, indicating the influence of photo-induced, dust surface-mediated reactions and resulting condensable vapor production. This study provides unique in situ observations of heterogeneous photochemical processes inducing new particle formation and growth in the real atmosphere, and suggests an unexpected impact of mineral dust on climate and atmospheric chemistry.

Aerosol particles, being important to both global climate^{1,2} and atmospheric chemistry³, can be directly emitted from natural or anthropogenic sources and secondarily formed in the atmosphere³. Mineral dust, with an emission rate of 1000–3000 Tg per year from deserts or semiarid areas⁴, is the most important primary aerosol particle source and dominates the aerosol mass in the global atmosphere. New particle formation (NPF) and subsequent particle growth form together a secondary aerosol particle source that controls the total particle number concentration^{5–7}. The climatic effects of mineral dust and atmospheric NPF have been thought to be disconnected from each other. Mineral dust affects climate via direct light scattering and ice nucleation^{1,2,8–10}, whereas NPF contributes significantly to the global cloud condensation nuclei (CCN) budget^{5–7} and thereby to uncertainties in the indirect radiative forcing^{11,12}.

Mineral dusts injected into the atmosphere can affect atmospheric photochemistry in very complicated ways. On one hand, dust tends to suppress photochemical processes via light scattering¹, scavenging of reactive gases¹³ and photochemical oxidant uptake^{14,15}. For example, both field and model studies have reported significant reductions of acidic gases and O₃ in dust plumes^{14,16–19}. On the other hand, recent studies indicate that mineral dust can induce chemical reactions in the presence of sunlight, defined as heterogeneous photochemistry^{20,21}. Such observations suggest that dust has the potential to participate in and promote the atmospheric photochemical processes directly as a reactant or catalyst²².

NPF and subsequent particle growth are tied to photochemistry as well. Particle nucleation generally originates from the production of H₂SO₄ via the oxidation of SO₂ by the OH radical⁵, while particle growth depends crucially on low-volatile vapors produced from the photo-oxidation of volatile organic compounds (VOCs)^{23,24}. High pre-existing particle loadings are considered to suppress the atmospheric NPF because of high condensation and coagulation sinks⁵. Therefore, it has been thought that dust and NPF do not usually co-exist, since high dust concentrations tend to scavenge both low-volatile vapors (e.g. sulfuric acid) and small molecular clusters efficiently^{6,7}. In this study, we analyzed a two-month period of comprehensive observations during the Asian dust storm season in 2009 at a mountain top site in southern China²⁵. The results show, for the first time, that high dust concentrations and NPF can really co-exist, in addition to



which we provide in situ evidence of dust-related heterogeneous photochemical processes that promote atmospheric new particle formation and growth.

Results

As a part of a field campaign on aerosol-cloud interaction at Mount Heng in Hunan Province, southern China²⁵, we conducted intensive measurements of a wide variety of trace gases and aerosols during spring 2009 (March to May), a season with frequent dust events (see Supplementary Information (SI) for details). Fig. 1 shows the temporal variation of several quantities (including PM_{10} , $PM_{2.5}$, calcium in $PM_{2.5}$, and particle number size distribution in the diameter range of 10–500 nm) measured during 20 April to 9 May, 2009. Two episodes of very high aerosol loadings, with maximum PM_{10} mass concentrations of about $248 \mu\text{g m}^{-3}$ and $911 \mu\text{g m}^{-3}$, appeared during 20–22 April and 25–26 April, respectively. The low mass fractions of fine particles and high calcium concentrations during the two events suggest the primary origin of these particles was a dust storm. The satellite observations on board the CALIPSO satellite on 25 April, showed clearly the presence of multi-layered dust aerosols in the lower troposphere over the southern China (Fig. S2).

Unexpectedly, intense new particle formation and growth was observed during the two major dust episodes (Fig. 1). The formation rates of 15 nm particles, J_{15} , were in general slightly higher during dust days than during non-dust days ($0.27 \pm 0.12 \text{ cm}^{-3} \text{ s}^{-1}$ vs. $0.23 \pm 0.06 \text{ cm}^{-3} \text{ s}^{-1}$), and the highest rate ($0.45 \text{ cm}^{-3} \text{ s}^{-1}$) was observed on the strongest dust day (April 25th, Table 1). It should be noted that J_{15} represents the combined effects of atmospheric nucleation, growth of nucleated particles to the diameter of 15 nm, and simultaneous scavenging of the growing nuclei by the pre-existing population of larger particles. As a result, J_{15} can be considered as a good metric for estimating the source rate of new particles that might eventually lead to the production of new CCN. The particle growth rates in the diameter range 15 to 30 nm were comparable to each other between the dust and non-dust days (Table 1), indicating larger production rates of extremely low-volatile vapors on dust days, when the condensation sink for such vapors was very high. In the diameter range 30 to 50 nm, the mean particle growth rate on dust days was $14.3 \pm 6.5 \text{ nm h}^{-1}$, more than twice the value on non-dust days (6.6

$\pm 3.4 \text{ nm h}^{-1}$). The highest growth rates were observed on April 22nd and 26th during the two main dust episodes (Table 1). Such growth rates are quite high compared to other regions around the world (typically below 10 nm h^{-1} in remote atmosphere and below 20 nm h^{-1} in some moderate polluted regions⁶). However, considering the high condensation and coagulation sinks at particle loadings in excess of $650 \mu\text{g m}^{-3}$ (mean value during the NPF period at 25th April), the occurrence of NPF and particle growth observed here appears to contradict our current understanding of aerosol dynamics^{5–7,11}.

Since sulfuric acid is the key driver of atmospheric nucleation^{5,26}, we utilized the sulfuric acid proxy approach, described simply as the ratio of $UV \times SO_2$ to condensation sink (CS)²⁷, to investigate the role of sulfuric acid in NPF events at Mt. Heng. Fig. 2A shows the scatter plot of $UV \times SO_2$ versus CS during typical (defined as continuous growth occurring after the particle nucleation) and non-typical NPF events (defined as no evident growth occurring after the particle nucleation, in which case particle nucleation rates and growth rates are hardly to be calculated) as well as non-NPF events. Since high sulfuric acid concentration and low CS promote NPF, it is not strange at all that the NPF event days (both typical and non-typical events) and non-NPF event days were separated into two different groups laying to the left and right of the diagonal line, respectively. However, the NPF events observed during 25–26 April behaved in the opposite way, especially on 25 April when the PM_{10} approached $650 \mu\text{g m}^{-3}$ at the period of NPF (12:00–14:59 LT). In addition, the formation of fine sulfate was observed during the dust event of 25–26 April (See strong diurnal cycle of sulfate in Fig. S7). Considering their alkaline nature, mineral dust particles should take up gaseous acids more easily than most other types of particles^{13,28}, which is expected to suppress NPF even further. Therefore, our observations strongly suggest an additional dust involved pathway enhancing the production of sulfuric acid. It should be noted that several recent studies in polluted urban regions also observed NPF with high CS²⁹, which can be attributed to even stronger source strength of low-volatile vapors resulting from very high SO_2 concentrations.

Particle growth plays a critical role in determining whether new-formed particles can reach sizes to be able to act as cloud condensation nuclei (diameter >50–100 nm). Different from particle nucleation,

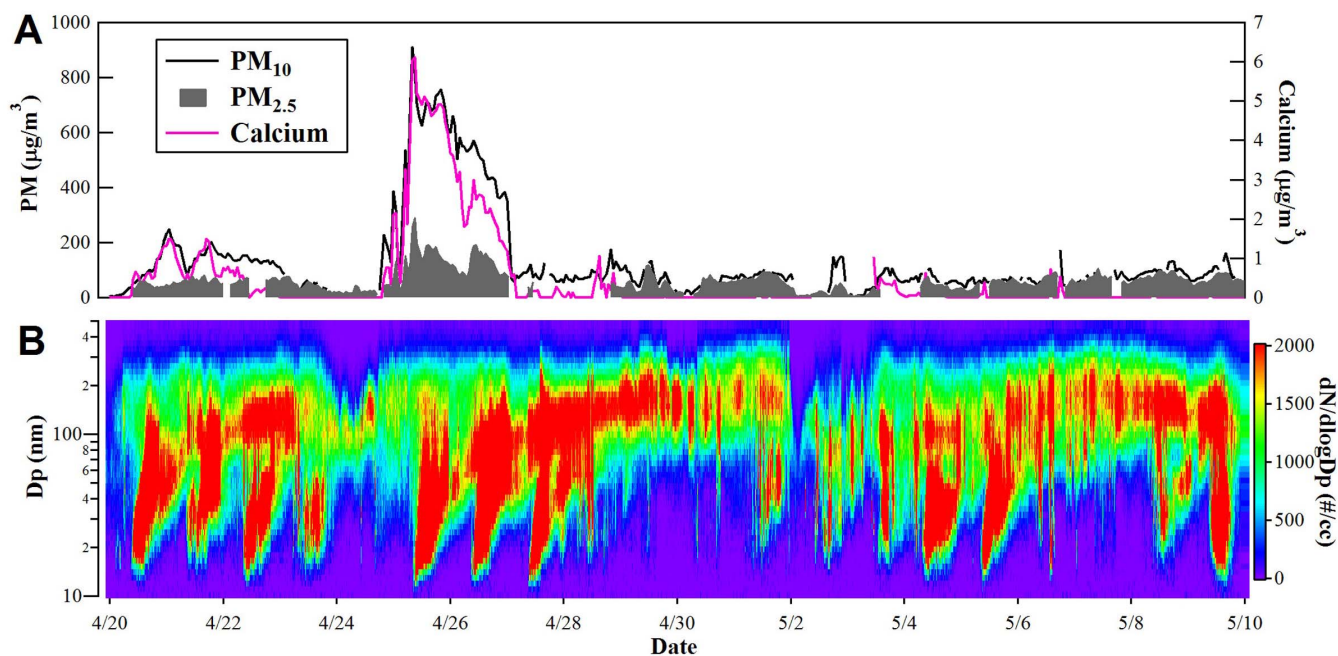


Figure 1 | Temporal variations of aerosol related parameters during 20 April to 9 May, 2009. (A) Time series of PM_{10} , $PM_{2.5}$, calcium in $PM_{2.5}$, and (B) particle number size distribution at Mt. Heng during April–May 2009.



Table 1 | Formation rates, growth rates, source rates of vapor and PM₁₀ concentrations during typical new particle formation events at Mt. Heng during March to May of 2009

Date	J _{1.5} * (cm ⁻³ s ⁻¹)	GR(15–30)* (nm h ⁻¹)	GR(30–50)* (nm h ⁻¹)	Q (cm ⁻³ s ⁻¹)	PM ₁₀ *** (μg m ⁻³)
15-Mar	0.26	4.3	NA**	1.0e + 06	****
25-Mar	0.17	5.6	5.6	1.1e + 06	56.3
7-Apr	0.27	7.7	11.4	1.9e + 06	75.7
20-Apr	0.15	6.1	6.1	1.0e + 06	82.0
22-Apr	0.20	4.9	19.3	1.5e + 06	135.1
25-Apr	0.45	7.2	12	2.8e + 06	668.6
26-Apr	0.26	7.4	22.4	2.8e + 06	506.9
27-Apr	0.31	6.1	11.9	1.7e + 06	75.3
4-May	0.17	4.6	3.5	1.3e + 06	69.8
5-May	0.29	6.4	5.8	1.8e + 06	54.6

*: The time periods of particle nucleation and growth varied largely from day to day. Generally, particle nucleation started at 10:00–12:00 LT, ended at 12:00–13:00 LT; particle growth from 15 nm to 30 nm started at 11:00–12:00 LT, ended at 13:00–14:00 LT; particle growth from 30 nm to 50 nm started at 13:30–14:30 LT, ended at 15:00–17:00 LT.

** : No growth rate can be detected.

*** : Hourly average values of 12:00–14:59 LT.

**** : PM₁₀ mass was not measured.

the contribution of sulfuric acid to particle growth is usually minor, especially at sizes larger than a few nanometers^{30,31}. Instead, low-volatile organic vapors (oxidized biogenic VOCs and nitrogen-containing organics) have demonstrated to play a key role^{23,24}. To investigate the possible roles of VOCs during the dust events, we estimated the concentration levels of directly-emitted VOCs during the campaign by carrying out Lagrangian dispersion modeling^{32–34} based on the emission inventories for total anthropogenic VOCs³⁵ and biogenic monoterpenes³⁶ (See Fig. S4). The simulations showed that, during the dust events, both anthropogenic and biogenic VOCs concentrations were much lower than the corresponding mean values during the whole campaign. In addition, the ratio of ozone concentration to CS, indicating the potential of producing high concentrations of low-volatile organic vapors, clearly showed much lower values during 25–26 April. This observation violates our current understanding of particle growth, unless there were some non-traditional mechanisms promoting the oxidation of VOCs.

So, what are the most plausible additional sources of gaseous sulfuric acid and low-volatile organic vapors? In case of sulfuric acid, one potential pathway is the dust-induced photo-catalytic reaction which can produce additional OH radicals to accelerate the oxidation of SO₂³⁷. This is a plausible explanation for the observed episode on 25–26 April, as the conditions with increased photo-sensitive

components, sufficient solar radiation, water and reactive species were favorable to this pathway. As shown in Fig. S5, the strongest new particle formation that occurred on 25 April was connected to heavy loadings of Fe (mostly exist as Fe₂O₃) and the highest relative humidity among the dust event days (detailed information is described in the SI, Fig. S5 and S6). Both of these features act in favor of heterogeneous photocatalytic reactions in the water films around the dust particles. In addition, the photolysis of enhanced HONO is another possible pathway to form OH radical, which has been demonstrated to be induced by the TiO₂ photocatalysis of NO₂ in our previous study^{25,38} (detailed information is also described in the SI).

In case of low-volatile organic vapors enhancing the particle growth, photo-promoted oxidation of VOCs by the illuminated dust, demonstrated by several laboratory studies^{39–41}, is considered as the most plausible pathway. Secondary vapors with a wide range of volatility can be produced by the oxidation of complex VOCs, such as biogenic organics. A small fraction of these vapors are extremely low volatile and can grow efficiently all-sized particles, including the very small ones⁴². Most of the oxidation products have higher volatilities and can contribute to the growth of larger particles only. Therefore, our observation that 30–50 nm particle growth rates were higher than those of 15–30 nm particles in the dust plumes (Table 1)

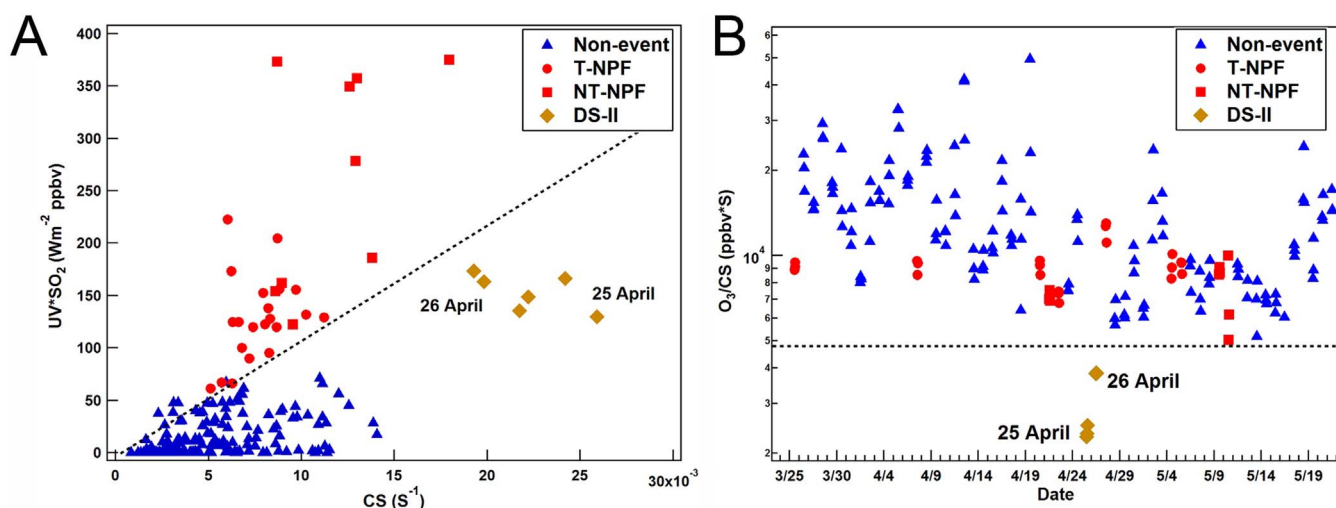


Figure 2 | Analysis of relationship between different proxies. (A) Scatter plot of hourly averaged UV × SO₂ versus condensation sink at noontime (12:00–14:59 LT), (B) Temporal variations of the ratios of daily noontime (12:00–14:59 LT) averaged ozone to condensation sink during March–May 2009.

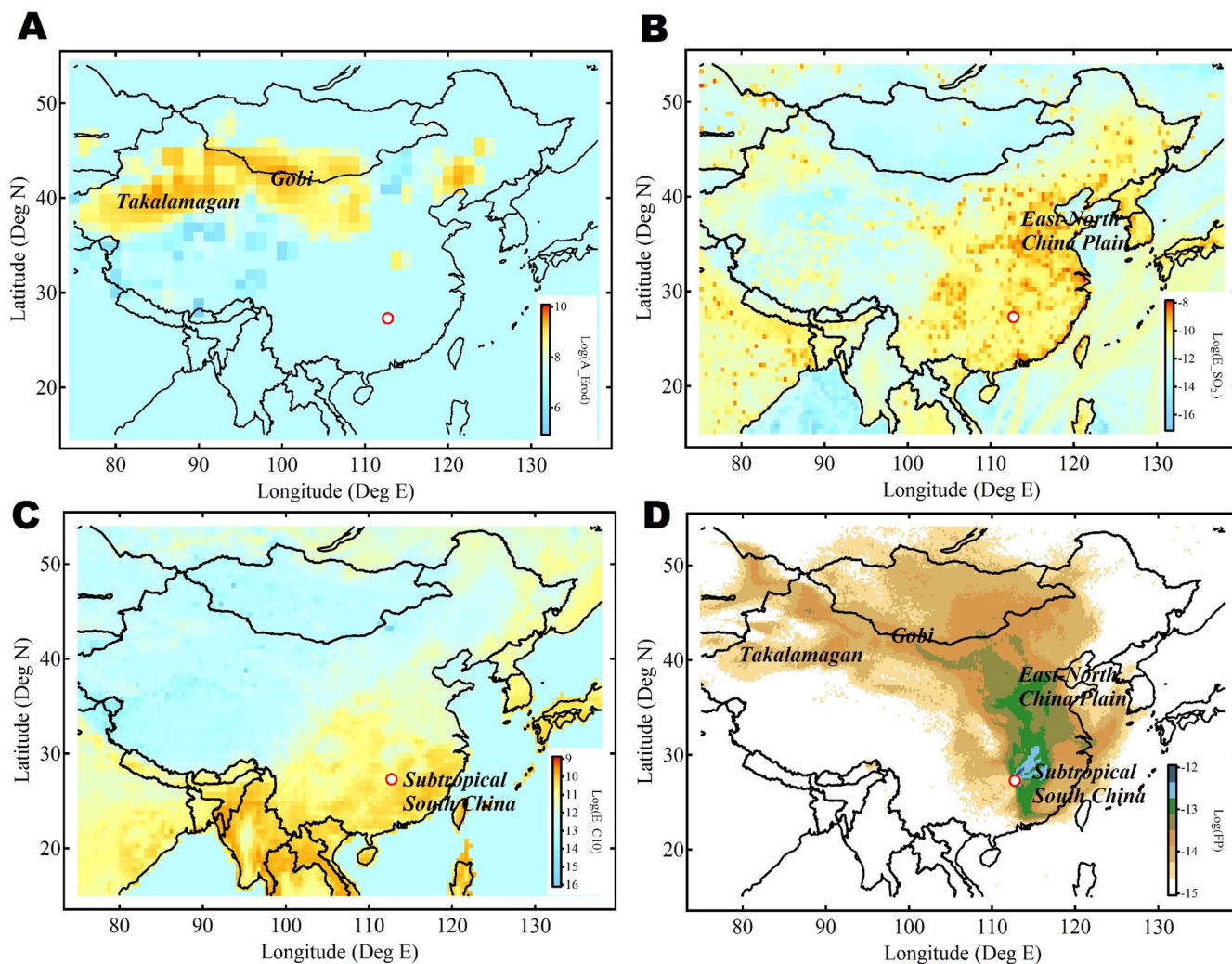


Figure 3 | Map shows eroded area, emission rates and transport pathways for the dust cases. (A) Area of eroded in Asia, (B) Emission rate of SO_2 , (C) Emission rate of monoterperene from biogenic emission in April, and (D) 100 m footprint retroplume calculated by 7-day backward Lagrangian dispersion simulation for 20–22 April and 25–26 April, 2009. The maps were drawn by the software of Igor Pro, <http://www.wavemetrics.com/>.

is consistent with our hypothesis of heterogeneous production of oxidants in dust plumes. To quantify the contribution of dust-related processes to the condensable vapors, we calculated the source rates of the vapors (Q) during the typical NPF days (see Table 1). During 25–26 April, the values of Q were $2.8 \times 10^6 \text{ cm}^{-3} \text{ s}^{-1}$, twice those on non-dust days (about $1.4 \times 10^6 \text{ cm}^{-3} \text{ s}^{-1}$ on average), indicating that at least half of the vapor precursors for observed particle growth on 25–26 April might have been produced from heterogeneous photochemical processes associated with the presence of dust.

In summary, our study provides observational evidence on photo-induced particle nucleation and growth, as well as HONO production²⁵, in the presence of mineral dust particles in the real atmosphere. These results demonstrate that mineral dust can participate in atmospheric photochemistry directly as reactants or catalysts, and that dust can enhance the atmospheric oxidation capacity by surface redox reactions²⁰ and gaseous radical production. Given the increasing evidence of anthropogenic industrial dust⁴³ and worldwide distribution of chromophores (i.e. nitrate and organics)²², photo-sensitive aerosols might be important to atmospheric photochemistry on a global scale. In laboratory experiments, dust-related heterogeneous photochemical reactions have been demonstrated to be stronger when dust particles are mixed or coated with other reactive species such as nitrate⁴⁴. In this study, such a mixture between mineral dust and anthropogenic pollutants actually occurred. In Fig. 3A–3D, we

show the calculated transport pathways using a Lagrangian transport and dispersion model with a “footprint” retroplume for the two events together with land-use data, maps of SO_2 emission and natural emission of monoterpenes. The analysis clearly shows that the observed air masses during the two dust events originated from the Taklimakan and Gobi Deserts and carried with the anthropogenic pollutants from the North China plain and eastern China to southern China. The time series in Fig. S5 show relatively high concentrations of anthropogenic pollutants (e.g. sulfate and BC in $\text{PM}_{2.5}$) during the dust events, suggesting a strong mix of dust and polluted plumes. This kind of mixed plumes provided abundant reactive species and water, which favored aging of the dust particles to form secondary coating (see Fig. S6), and induced heterogeneous photochemical reactions during the long range transport²⁵. For example, the photodecomposition of coated nitrate may release NO_3 radical to oxidize some specific VOCs⁴⁴ (Detailed descriptions are in the SI).

Discussion

Our investigation provides “direct” observational evidence on new particle formation and growth in heavy dust plumes mixed with anthropogenic pollution, and suggests an unexpected source of nucleating and condensable vapors via dust-induced heterogeneous photochemical processes. In Asia, huge amounts of dust is being produced during the dry season from both Gobi and Taklimakan

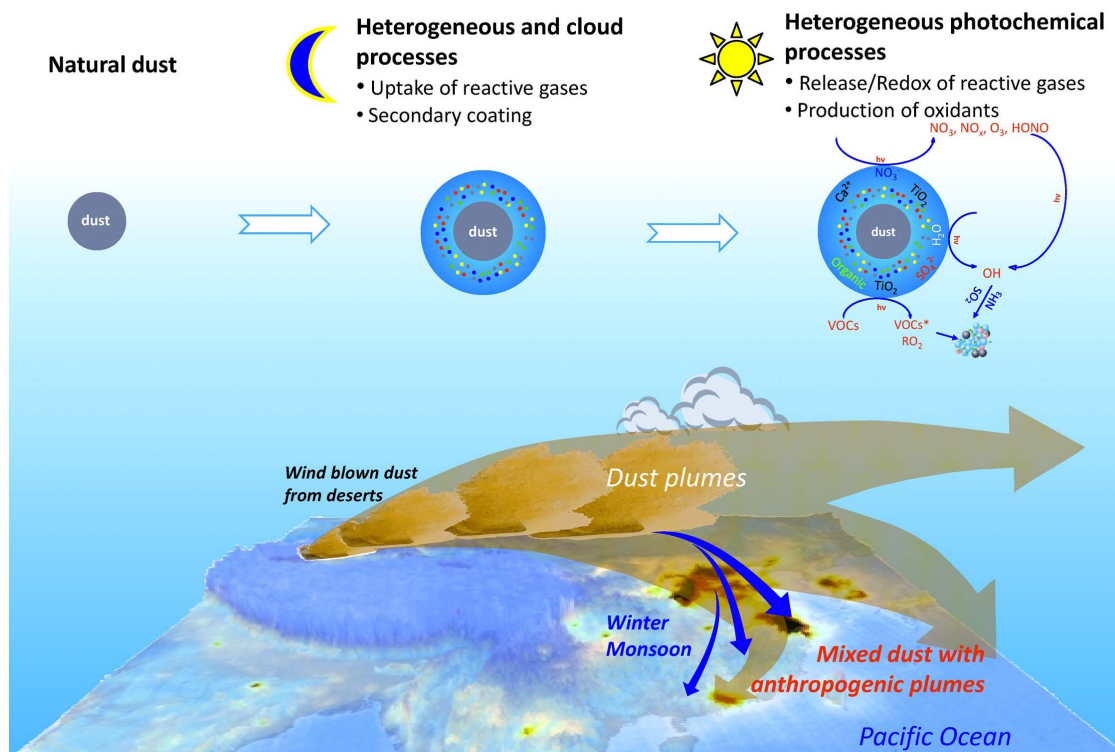


Figure 4 | Schematic description of main stages of Asian dusts during the long range transport in the atmosphere and their main transport pathways. Stage I—Mineral dusts are injected into the atmosphere in the remote area. Stage II—dust particles uptake anthropogenic reactive gases and form secondary coatings after they are transported over areas with high anthropogenic emissions. Heterogeneous photochemical processes should play a role in this stage, but they are easily covered up by strong gas phase photochemistry. Stage III—aged dusts transport to the remote Asia-Pacific region, where the plumes experience heterogeneous photochemical reactions favoring the new particle formation and growth. The map in the figure was drawn by Global Mapper.

deserts^{45,46}, and the dust is being transported eastward across the polluted northern and eastern parts of China (Fig. 4). The mixture of dust and anthropogenic pollution plumes can be further transported easterly in the mid-troposphere and southerly in the lower-troposphere, causing significant impacts on the remote atmosphere in downwind areas like the Pacific Ocean even other continents in the world^{47,48} (Fig. 4). Given that the polluted dust promotes new particle formation and growth, this study suggests a more crucial role of dust in both regional and global climate change than the current knowledge suggests. In addition, the observation of dust-promoted particle nucleation and growth, along with HONO production, provides strong evidence on the role of aerosol-related photochemistry, which would enhance the atmospheric oxidation capacity via photo-induced surface redox reactions and gaseous radical production (Fig. 4). These findings challenge the traditional point of view that aerosols are net sinks for the atmospheric oxidation capacity, and indicate a possible pathway for the large missing source of OH radical in heavily polluted regions⁴⁹.

Methods

Field experiment. Mount Heng located in the middle of Hunan Province, southern China, is a remote mountain area with few local sources around but generally downwind both source regions of Asia dusts and anthropogenic pollutions in the spring (Fig. S5). The field campaign was conducted March to May in 2009 at a meteorological station on the summit of Mt. Heng. Comprehensive parameters of trace gases and aerosol components, including SO₂, O₃, PM_{2.5}, PM₁₀, sulfate, calcium, BC in PM_{2.5}, were continuously measured during the campaign. Particle number size distributions in the range of 10–10000 nm were employed to detect the particle nucleation and growth. Several filter-based samples were also collected and analyzed to assist in interpreting the observed phenomena. Detailed information is provided in the SI.

Numerical calculation and modeling. Methods to calculate the particle formation rates, growth rates, and condensation sink (CS) are followed the suggestion of

Kulmala et al.⁵⁰. Lagrangian particle dispersion modeling (LPDM) was carried out based on a method developed and evaluated by Ding et al.⁵² using the Hybrid Single-Particle Lagrangian Integrated Trajectory (HYSPRIT) model. For each hour, 3000 particles were released at the site and were traced backward for a 7-day period. The residence time at 100 m altitude, i.e. footprint retroplumes, were used to understand the contribution from potential source regions.

1. IPCC. Climate change 2013: the physical science basis. Contribution of working group I to the fifth assessment report of the intergovernmental panel on climate change. Stocker, T. F. et al. (eds.). Cambridge University Press, Cambridge, United Kingdom and New York, NY, USA, (2013).
2. Ramanathan, V., Crutzen, P. J., Kiehl, J. T. & Rosenfeld, D. Aerosols, climate, and the hydrological cycle. *Science* **294**, 2119–2124 (2001).
3. Seinfeld, J. H. & Pandis, S. N. *Atmospheric chemistry and physics: from air pollution to climate change*. (John Wiley & Sons, 2006).
4. Tegen, I. & Schepanski, K. The global distribution of mineral dust. *IOP Conference Series: Earth and Environmental Science* **7**, Barcelona, Spain. Bristol, United Kingdom: IOP Publishing, 012001 (2009).
5. Kulmala, M. et al. On the formation, growth and composition of nucleation mode particles. *Tellus B* **53**, 479–490 (2001).
6. Kulmala, M. et al. Formation and growth rates of ultrafine atmospheric particles: a review of observations. *J. Aerosol Sci.* **35**, 143–176 (2004).
7. Zhang, R., Khalizov, A., Wang, L., Hu, M. & Xu, W. Nucleation and growth of nanoparticles in the atmosphere. *Chem. Rev.* **112**, 1957–2011 (2012).
8. Andreae, M. O. & Crutzen, P. J. Atmospheric aerosols: biogeochemical sources and role in atmospheric chemistry. *Science* **276**, 1052–1058 (1997).
9. Zhu, A., Ramanathan, V., Li, F. & Kim, D. Dust plumes over the Pacific, Indian, and Atlantic oceans: climatology and radiative impact. *J. Geophys. Res.* **112**, D16208 (2007).
10. Li, F., Vogelmann, A. M. & Ramanathan, V. Saharan dust aerosol radiative forcing measured from space. *J. Climate* **17**, 2558–2571 (2004).
11. Kazil, J. et al. Aerosol nucleation and its role for clouds and Earth's radiative forcing in the aerosol-climate model ECHAM5-HAM. *Atmos. Chem. Phys.* **10**, 10733–10752 (2010).
12. Makkonen, R. et al. BVOC-aerosol-climate interactions in the global aerosol-climate model ECHAM5.5-HAM2. *Atmos. Chem. Phys.* **12**, 10077–10096 (2012).
13. Usher, C. R., Michel, A. E. & Grassian, V. H. Reactions on mineral dust. *Chem. Rev.* **103**, 4883–4939 (2003).



14. de Reus, M. *et al.* Airborne observations of dust aerosol over the North Atlantic Ocean during ACE 2: indications for heterogeneous ozone destruction. *J. Geophys. Res.* **105**, 15263–15275 (2000).
15. Hanisch, F. & Crowley, J. N. Ozone decomposition on Saharan dust: an experimental investigation. *Atmos. Chem. Phys.* **3**, 119–130 (2003).
16. Zhang, Y., Sunwoo, Y., Kotamarthi, V. & Carmichael, G. R. Photochemical oxidant processes in the presence of dust: an evaluation of the impact of dust on particulate nitrate and ozone formation. *J. Appl. Meteorol. Clim.* **33**, 813–824 (1994).
17. Bauer, S. E., Balkanski, Y., Schulz, M., Hauglustaine, D. A. & Dentener, F. Global modeling of heterogeneous chemistry on mineral aerosol surfaces: influence on tropospheric ozone chemistry and comparison to observations. *J. Geophys. Res.* **109**, D02304 (2004).
18. Tang, Y. *et al.* Impacts of dust on regional tropospheric chemistry during the ACE-Asia experiment: a model study with observations. *J. Geophys. Res.* **109**, D19S21 (2004).
19. Fairlie, T. D. *et al.* Impact of mineral dust on nitrate, sulfate, and ozone in transpacific Asian pollution plumes. *Atmos. Chem. Phys.* **10**, 3999–4012 (2010).
20. Ndour, M., Conchon, P., D'Anna, B., Ka, O. & George, C. Photochemistry of mineral dust surface as a potential atmospheric renoxification process. *Geophys. Res. Lett.* **36**, L05816 (2009).
21. Monge, M. a. E. *et al.* Ozone formation from illuminated titanium dioxide surfaces. *J. Am. Chem. Soc.* **132**, 8234–8235 (2010).
22. Cwiertny, D. M., Young, M. A. & Grassian, V. H. Chemistry and photochemistry of mineral dust aerosol*. *Annu. Rev. Phys. Chem.* **59**, 27–51 (2008).
23. Donahue, N. M., Trump, E. R., Pierce, J. R. & Riipinen, I. Theoretical constraints on pure vapor-pressure driven condensation of organics to ultrafine particles. *Geophys. Res. Lett.* **38**, L16801 (2011).
24. Riipinen, I. *et al.* Organic condensation: a vital link connecting aerosol formation to cloud condensation nuclei (CCN) concentrations. *Atmos. Chem. Phys.* **11**, 3865–3878 (2011).
25. Nie, W. *et al.* Asian dust storm observed at a rural mountain site in southern China: chemical evolution and heterogeneous photochemistry. *Atmos. Chem. Phys.* **12**, 11985–11995 (2012).
26. Kulmala, M. *et al.* Direct observations of atmospheric aerosol nucleation. *Science* **339**, 943–946 (2013).
27. Petäjä, T. *et al.* Sulfuric acid and OH concentrations in a boreal forest site. *Atmos. Chem. Phys.* **9**, 7435–7448 (2009).
28. Dentener, F. J., Carmichael, G. R., Zhang, Y., Lelieveld, J. & Crutzen, P. J. Role of mineral aerosol as a reactive surface in the global troposphere. *J. Geophys. Res.* **101**, 22869–22889 (1996).
29. Yue, D. *et al.* Characteristics of aerosol size distributions and new particle formation in the summer in Beijing. *J. Geophys. Res.* **114**, D00G12 (2009).
30. Fiedler, V. *et al.* The contribution of sulphuric acid to atmospheric particle formation and growth: a comparison between boundary layers in Northern and Central Europe. *Atmos. Chem. Phys.* **5**, 1773–1785 (2005).
31. Kuang, C. *et al.* An improved criterion for new particle formation in diverse atmospheric environments. *Atmos. Chem. Phys.* **10**, 8469–8480 (2010).
32. Ding, A., Wang, T. & Fu, C. Transport characteristics and origins of carbon monoxide and ozone in Hong Kong, South China. *J. Geophys. Res.* **118**, 9475–9488 (2013).
33. Ding, A. J. *et al.* Ozone and fine particle in the western Yangtze River Delta: an overview of 1 yr data at the SORPES station. *Atmos. Chem. Phys.* **13**, 5813–5830 (2013).
34. Zhang, J. M. *et al.* Continuous measurement of peroxyacetyl nitrate (PAN) in suburban and remote areas of western China. *Atmos. Environ.* **43**, 228–237 (2009).
35. Zhang, Q. *et al.* Asian emissions in 2006 for the NASA INTEX-B mission. *Atmos. Chem. Phys.* **9**, 5131–5153 (2009).
36. Guenther, A. *et al.* Estimates of global terrestrial isoprene emissions using MEGAN (Model of Emissions of Gases and Aerosols from Nature). *Atmos. Chem. Phys.* **6**, 3181–3210 (2006).
37. Dupart, Y. *et al.* Mineral dust photochemistry induces nucleation events in the presence of SO₂. *Proc. Natl. Acad. Sci. USA* **109**, 20842–20847 (2012).
38. Ndour, M. *et al.* Photoenhanced uptake of NO₂ on mineral dust: laboratory experiments and model simulations. *Geophys. Res. Lett.* **35**, L05812 (2008).
39. Marci, G. *et al.* Photocatalytic oxidation of toluene on irradiated TiO₂: comparison of degradation performance in humidified air, in water and in water containing a zwitterionic surfactant. *J. Photoch. Photobio. A.* **160**, 105–114 (2003).
40. Chen, H., Nanayakkara, C. E. & Grassian, V. H. Titanium dioxide photocatalysis in atmospheric chemistry. *Chem. Rev.* **112** (2012).
41. Monge, M. E. *et al.* Alternative pathway for atmospheric particles growth. *Proc. Natl. Acad. Sci. USA* (2012).
42. Ehn, M. *et al.* A large source of low-volatility secondary organic aerosol. *Nature* **506**, 476–479 (2014).
43. Vicki, H. G. New directions: nanodust – a source of metals in the atmospheric environment? *Atmos. Environ.* **43**, 4666–4667 (2009).
44. Styler, S. A. & Donaldson, D. J. Photooxidation of atmospheric alcohols on laboratory proxies for mineral dust. *Environ. Sci. Technol.* **45**, 10004–10012 (2011).
45. Zhang, X. Y., Arimoto, R. & An, Z. S. Dust emission from Chinese desert sources linked to variations in atmospheric circulation. *J. Geophys. Res.* **102**, 28041–28047 (1997).
46. Formenti, P. *et al.* Recent progress in understanding physical and chemical properties of African and Asian mineral dust. *Atmos. Chem. Phys.* **11**, 8231–8256 (2011).
47. Parrington, J. R., Zoller, W. H. & Aras, N. K. Asian dust: seasonal transport to the Hawaiian Islands. *Science* **220**, 195–197 (1983).
48. Jacob, D. J. *et al.* Transport and chemical evolution over the Pacific (TRACE-P) aircraft mission: design, execution, and first results. *J. Geophys. Res.* **108**, 9000 (2003).
49. Hofzumahaus, A. *et al.* Amplified trace gas removal in the troposphere. *Science* **324**, 1702–1704 (2009).
50. Kulmala, M. *et al.* Measurement of the nucleation of atmospheric aerosol particles. *Nat. Protoc.* **7**, 1651–1667 (2012).

Acknowledgments

Data analysis of this work was supported the NSFC projects (D03/41321062 and D0512/0207131138) and the MOST 973 project (2010CB428500). The field campaign was supported by the MOST 973 Project (2005CB422203). Part of the work by Nie Wei was supported by the Hong Kong Polytechnic University. Part of this work was also supported by the Jiangsu Provincial Science Fund for Distinguished Young Scholars awarded by A. Ding (No. BK20140021) and the Centre of Excellence in Atmospheric Science in Finland. We thank the Mt. Heng Observatory for providing the measurement platform for this campaign. The emission inventories were provided by ECCAD (The GEIA Database) and Q. Zhang at Tsinghua University, and the CALIPSO data were provided by LARC of NASA. The authors would like to thank Douglas R. Worsnop at Aerodyne Research Inc, Abdelwahid Mellouki at CNRS, Hartmut Herrmann at TROPOS, Minghui Wang at PNNL, and Yafang Cheng and Hang Su at MPIC for their useful suggestions and comments.

Author contributions

A.D., T.W., W.W. and M.K. lead the overall scientific questions. W.N. participated in the field measurement and contributed to data analysis. V.K., C.G., T.P., X.Y., C.F. and M.K. involved in initial discussions, and commented and edited the manuscript. X.Q. contributed to the data analysis. L.X., Q.Z., X.G. and X.W. participated the campaign and operated some trace gases and PM instruments. Correspondence and requests for materials should be addressed to A.D. (dingaj@nju.edu.cn) or T.W. (tao.wang@polyu.edu.hk)

Additional information

Supplementary Information accompanies this paper at <http://www.nature.com/scientificreports>

Competing financial interests: The authors declare no competing financial interests.

How to cite this article: Nie, W. *et al.* Polluted dust promotes new particle formation and growth. *Sci. Rep.* **4**, 6634; DOI:10.1038/srep06634 (2014).



This work is licensed under a Creative Commons Attribution-NonCommercial-ShareAlike 4.0 International License. The images or other third party material in this article are included in the article's Creative Commons license, unless indicated otherwise in the credit line; if the material is not included under the Creative Commons license, users will need to obtain permission from the license holder in order to reproduce the material. To view a copy of this license, visit <http://creativecommons.org/licenses/by-nc-sa/4.0/>